PHYSICAL REVIEW B **85**, 045402 (2012)

Material- and geometry-independent multishell cloaking device

Pattabhiraju C. Mundru, Venkatesh Pappakrishnan, and Dentcho A. Genov*
College of Engineering and Science, Louisiana Tech University, Ruston, Louisiana 71270, USA
(Received 4 November 2011; revised manuscript received 12 December 2011; published 3 January 2012)

In this paper we propose a multishell generic cloaking system. A transparency condition independent of the object's optical and geometrical properties is proposed in the quasistatic regime of operation. The suppression of dipolar scattering is demonstrated in both cylindrically and spherically symmetric systems. A realistic tunable low-loss shell design is proposed based on a composite metal-dielectric shell. The effects due to dissipation and dispersion on the overall scattering cross section are thoroughly evaluated. It is shown that a strong reduction of scattering by a factor of up to 10^3 can be achieved across the entire optical spectrum. Full wave numerical simulations for complex shaped particles are performed validating the analytical theory. The proposed design does not require optical magnetism and is generic in the sense that it is independent of the object's material and geometrical properties.

DOI: 10.1103/PhysRevB.85.045402 PACS number(s): 78.66.Sq, 78.20.Bh, 78.20.Ci

I. INTRODUCTION

Recently, *cloaking* or *invisibility* has received significant attention from the scientific community. Several methods have been proposed to cloak macroscopic and microscopic objects: Transformation optics (TO)[1–12] and elimination of dipolar scattering[13–15] are widely used. Both of these approaches are based on engineering a specific material shell(s) around an object to render it invisible for external observers.

In 2006, Leonhardt[3] used optical conformal mapping to design an isotropic cloaking design with spatially dependent refractive index around an object, achieving invisibility in the ray approximation. Pendry *et al.*[4] proposed the TO approach in order to design an electromagnetic metamaterial (EMM) shell that bends light rays and conformably transfers the wave fronts around an object. Using TO, Lai *et al.*[7] designed a complementary media[8] that can conceal objects placed at a distance outside the cloaking system from electromagnetic radiation. McCall *et al.*,[10] by transforming both space and time, reported a space-time cloak (STC) design that can hide events rather than objects. In contrast to spatial transformation cloaks which bend light around a finite region of space, STC works on the variation of the velocity of light before and after the occurrence of the event to be cloaked and its realization demands sophisticated temporal EMM designs. The EMMs are artificial materials engineered with desired electromagnetic properties that are difficult or impossible to find in nature. The remarkable properties of these materials are responsible for developing novel optical systems with negative refractive index media,[16] lensing with super-resolution,[17] cloaking devices,[11] and systems that create an optical illusion such that an object can appear to an external observer with entirely different characteristics.[18] Furthermore, EMMs have been used to mold the flow of light at will,[19,20] functionalities that are virtually impossible to achieve with naturally available materials.

Electromagnetic invisibility through elimination of dipolar scattering was studied decades ago by Kerker[14] in the case of a subwavelength ellipsoidal object. More recently, a similar study in the case of spherical and cylindrical geometries was presented by Alù and Engheta.[13] In these studies a reduction in the total scattering cross section was demonstrated by using dielectric shells with appropriately configured geometrical and optical properties. Zhou and Hu[15] furthered this concept by using the idea of *neutral inclusion* to derive the generalized transparency condition in quasistatic limit. However, all these studies place explicit geometrical and material constraints upon the shells of the cloaking system as well as the object. These constraints make the cloak crucially dependent on the optical and geometrical properties of the object and arguably limit its applicability.

In this paper, we propose a multishell design that can cloak an object regardless of its shape and material (optical) properties in the quasistatic regime. A set of transparency conditions independent of the object are derived for both cylindrically and spherically symmetric systems. Most importantly, as a material realization of our system, we propose a *zero-index, low-loss, tunable* shell design based on metal-dielectric composite materials. Our results show that the proposed design can achieve cloaking across the entire optical spectral range and can decrease the scattering cross section by a factor up to 10^3. In addition, full wave analysis performed for a two-dimensional or cylindrically symmetric system shows the object independence of the design in good agreement with the developed analytical theory.

The rest of the paper is organized as follows. Section II outlines the transparency conditions for a multishell cloaking system independent of the object's optical and geometrical properties. Section III analyzes the behavior of the cloak based on realistic shells, i.e., shells made of dispersive materials (bulk metal and metal-dielectric composites), and compares the results to the ideal lossless case. Section IV provides a time varying and finite difference frequency domain (FDFD) analysis of our cloaking system.

II. THEORETICAL ANALYSIS

The geometry of the problem is depicted in Fig. 1. An object of arbitrary shape and permittivity ε_0 is placed inside a cylindrical or spherical domain of radius r_0 (core) surrounded by a system of l shells of radii $r_1, r_2, \ldots, r_l$ ($r_0 < r_1 < r_2 \cdots r_l$) and permittivities $\varepsilon_1, \varepsilon_2, \ldots, \varepsilon_l$, respectively. The cloak is embedded in a medium with permittivity ε_e and illuminated by a uniform electric field E_0 polarized along $+x$ axis [or

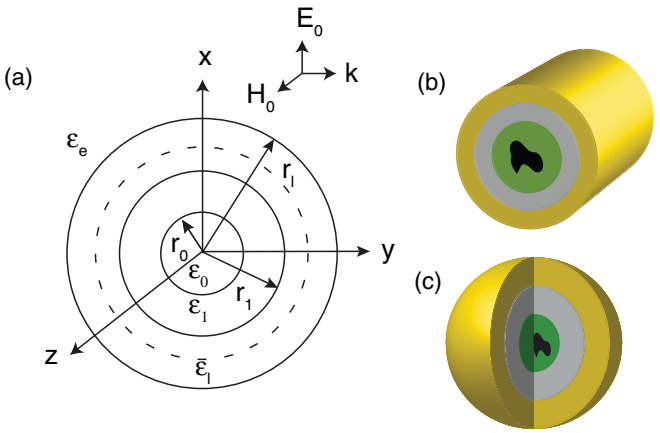

FIG. 1. (Color online) (a) Generic multishell cloaking system with shell radii r_i and permittivity ε_i, a two-shell (b) cylindrically symmetric cloaking system and (c) spherically symmetric cloaking system.

transfer magnetic (TM) wave]. In the quasistatic limit, the electric potential inside and outside the cloak can be written as

$$\varphi_{2D} = E_0 \sum_{n=1}^{\infty} \left(A_n^{2D} r^n + S_n^{2D} r^{-n}\right) \cos(n\phi), \tag{1}$$

$$\varphi_{3D} = E_0 \sum_{n=1}^{\infty} \left(A_n^{3D} r^n + S_n^{3D} r^{-(n+1)}\right) P_n[\cos(n\phi)], \tag{2}$$

where A_n^d, S_n^d are amplitude coefficients, P_n are the associated Legendre polynomials, and d is the dimensionality. On applying tangential and normal boundary conditions at r_0, r_1, $r_2, \ldots, r_l$, the dipolar terms ($n = 1$) responsible for the far field scattering in the embedding media can be written as

$$S_1^d = r_l^d \frac{\varepsilon_{\text{eff}}^l - \varepsilon_e}{\varepsilon_{\text{eff}}^l + (d-1)\varepsilon_e}, \tag{3}$$

where

$$\varepsilon_{\text{eff}}^l = \varepsilon_l + \frac{d\varepsilon_l p_l \left(\varepsilon_{\text{eff}}^{l-1} - \varepsilon_l\right)}{d\varepsilon_l + (1-p_l)\left(\varepsilon_{\text{eff}}^{l-1} - \varepsilon_l\right)} \tag{4}$$

is the effective permittivity of the $l-$shell system, and $p_l = (r_{l-1}/r_l)^d$ are the shells surface to volume ratios. We must note that using the natural condition $\varepsilon_{\text{eff}}^0 = \varepsilon_0$, Eqs. (3) and (4) provide a straightforward recurrence formula for estimating the scattering coefficient of multilayered dielectric particles in the quasistatic approximation without explicitly solving the boundary value problem (see Appendix for more details). This rendering of the problem also gives an intuitive understanding of the scattering process as that of an equivalent spherical and/or cylindrical particle with effective permittivity $\varepsilon_{\text{eff}}^l$ immersed in a host environment with permittivity ε_e.

Alù and Engheta[13] and Zhou and Hu[15] have shown that, in the quasistatic limit, complete elimination of dipolar scattering can be achieved by a proper choice of the shell(s) radii. Following their hypothesis, in the limit $S_1^d \to 0$ ($\varepsilon_{\text{eff}}^l = \varepsilon_e$) we obtain a general transparency condition for the $l-$shell cloaking system which depends on the object permittivity and size:

$$p_l = \left(\frac{\varepsilon_l - \varepsilon_e}{\varepsilon_l - \varepsilon_{\text{eff}}^{l-1}}\right)\left[\frac{\varepsilon_{\text{eff}}^{l-1} + (d-1)\varepsilon_l}{\varepsilon_e + (d-1)\varepsilon_l}\right], \quad (l \geqslant 1). \tag{5}$$

The condition in Eq. (5) is consistent with the transparency conditions reported in Refs. 13 and 15 for single-shell and two-shell geometries. Specifically, for $l = 1$ and $d = 3$, i.e., a single-shell spherically symmetric cloak, Eq. (5) reduces to the condition reported by Alù and Engheta:[13]

$$p_1 = \left(\frac{r_0}{r_1}\right)^3 = \frac{(\varepsilon_1 - \varepsilon_e)(2\varepsilon_1 + \varepsilon_0)}{(\varepsilon_1 - \varepsilon_0)(2\varepsilon_1 + \varepsilon_e)}, \tag{6}$$

where ε_1 is the shell permittivity. As evident from Eq. (6) this design does not require high refractive indices or optical magnetism as in the case of transformational optics (TO).[12] However, realizations of such cloaking systems present a serious disadvantage; redesign of the entire cloak is necessitated for any change in the object's properties (ε_0 and r_0 are the permittivity and radius of the object), and it is applicable only for spherically and/or cylindrically symmetric objects.

Alternatively, here we propose a different condition to achieve complete elimination of dipolar scattering for a cloak with $l \geqslant 2$ shells. By inspection [see Eqs. (3) and (4)] this is achieved ($\varepsilon_{\text{eff}}^l = \varepsilon_e$) if the two outermost cloaking shells have permittivities that satisfy the following conditions:

$$\varepsilon_{l-1} = 0, \quad \varepsilon_l = \varepsilon_e \frac{1 + p_l/(d-1)}{1 - p_l}. \tag{7}$$

Provided a zero-index material can be designed the permittivity of the outermost shell is dependent only on the radii of the lth, and $(l-1)$th shells, which is in sharp contrast with the transparency condition given by Eqs. (5), and (6). Thus, in the quasistatic limit, a cloaking system parametrized by the transparency condition Eq. (7) has the potential to cloak objects with arbitrary optical properties. Furthermore, as will be demonstrated in Sec. IV, the conditions $\varepsilon_{l-1} \to 0$ allow cloaking of objects with arbitrary shapes provided they are immersed within shells of order lower than $l-1$. Interestingly, a striking similarity exists between the cloak designs based on our approach and those on conventional transformation optics. In the case of transformation optics, perfect cloaking can be achieved provided the permittivity or/and permeability of the anisotropic shell is zero at the boundary between the shell and the object.[6] Zero-index materials correspond to a situation where the local electromagnetic field does not experience phase shift as it travels through the material. In the case of cloaking this also implies a singular value of the local wavelength ($\lambda \to \infty$) or an effective size of the object equal to zero. This explains why in the case of transformation optics and under the here-proposed transparency condition Eq. (7), the invisibility devices operate independently of the object geometrical or/and material properties. An object with effective size equal to zero does not interact with the impinging light. For the here-proposed cloak, the simplest realization is the two-shell design.

III. CLOAK DESIGN AND TUNABILITY

A. Metallic shell design

We consider two-shell cylindrical and spherical cloaking systems [see Figs. 1(b) and 1(c)] with air ($\varepsilon_e = 1$) as environment. To satisfy the transparency condition, Eq. (7), we utilize a metallic inner shell. The metal permittivity is described by the Drude model, $\varepsilon_m(\omega) = \varepsilon'_m(\omega) + i\varepsilon''_m(\omega) = \varepsilon_b - {\omega_p}^2/\omega(\omega + i\omega_\tau)$, where ω_p is plasma frequency, ω_τ is relaxation rate, and ε_b is contribution due to interband transitions. Clearly, at the modified plasma frequency $\tilde{\omega}_p = \omega_p/\sqrt{\varepsilon_b}$, the metal permittivity $\varepsilon'_m(\tilde{\omega}_p) = 0$ (for $\omega_\tau/\tilde{\omega}_p \ll 1$) and a metal shell can be used to implement the cloak. To characterize the cloak performance we define the relative scattering length (RSL), for the cylindrical case $d = 2$, and relative scattering cross section (RSCS) for spherically symmetric case $d = 3$ as

$$\sigma_R^d = \frac{\sigma_{\text{cloak}}^d}{\sigma_{\text{object}}^d} = \frac{\left|S_{1,\text{cloak}}^d\right|^2}{\left|S_{1,\text{object}}^d\right|^2}, \tag{8}$$

where σ_{cloak}^d and σ_{object}^d are the scattering length (scattering cross section) of the cloak and object, respectively. Substituting the transparency condition Eq. (7) in Eq. (3) and using $\varepsilon_2 = \varepsilon_m(\tilde{\omega}_p) = i\varepsilon''_m(\tilde{\omega}_p)$ (here ε''_m is the imaginary part of the metal permittivity) in the second order of the small parameter $\varepsilon''_m \approx \varepsilon_b\omega_\tau/\tilde{\omega}_p \ll 1$ we obtain

$$\sigma_R^d(\tilde{\omega}_p) \approx \left[\frac{d\varepsilon''_m(\tilde{\omega}_p)}{p_1}\right]^2 \left\{\frac{(\varepsilon_0 + d - 1)\,[1 + (d-1)p_1]}{(\varepsilon_0 - 1)(1 - p_1)(p_2 + d - 1)^2}\right\}^2. \tag{9}$$

The existence of material dissipation clearly affects the cloak performance with $\sigma_R^d \approx (\omega_\tau/\omega_p)^2$ increasing quadratically with the relaxation rate ω_τ. Furthermore, inspection of Eq. (9) shows that a geometrical optimization could be archived with the scattering having a minimum for $p_1 = 1/(1 + \sqrt{d})$. Finally, using Eq. (7) the optimal RSL and RSCS can be written as a function of the outer-shell permittivity:

$$\sigma_{R,\min}^d(\tilde{\omega}_p) \approx \varepsilon_b^3 \left(\frac{\omega_\tau}{\omega_p}\right)^2 \left[\frac{(\varepsilon_0 + d - 1)(d - 1 + 1/\varepsilon_2)^2}{d(\varepsilon_0 - 1)(1 - \sqrt{d})^2}\right]^2. \tag{10}$$

To demonstrate the cloak performance we consider two separate designs for the cylindrical and spherical geometries. Due to lower dissipative losses, we chose silver with $\hbar\omega_p = 9.1$ eV, $\hbar\omega_\tau = 0.02$ eV, and $\varepsilon_b = 5$.[21] The cloak's performances calculated as a function of the outer-shell permittivity ε_2 are shown in Fig. 2. For comparison, we include the RSL and RSCS of the ideal systems (without dissipative losses) and with a silver inner shell. The RSL and RSCS of the ideal systems approach zero, implying *perfect invisibility* at the outer-shell permittivity values $\varepsilon_2 = 5$ and $\varepsilon_2 = 10$ in cases I and II (see Fig. 2), for cylindrical and spherical geometries. These results are in excellent agreement with the values predicted by the transparency condition Eq. (7). A significant reduction in scattering for the metal shell systems are also observed at the predicted outer-shell dielectric permitivities ε_2 (see Fig. 2, dashed lines). In the figures we have also included the minimal RSL and RSCS as given by Eq. (10), providing a guideline of the maximal affects that can be achieved with the proposed design. At the optimal outer-shell permittivity the exact result correlates well with the predicted values, and for strongly scattering objects ($\varepsilon_0 \to \infty$) asymptotically approach the limit $\sigma_{\text{RSCS}}^{\min} \to \varepsilon_b^3(\omega_\tau/\omega_p)^2(1 + 1/\sqrt{d})^4 \ll 1$. Finally, we must note that the cloak based on the metal shell design inherently has a rather narrow frequency range of operation. The operation range $\omega \in (\tilde{\omega}_p - \Delta\omega, \tilde{\omega}_p + \Delta\omega)$ is roughly set by the condition $|\varepsilon'_m(\tilde{\omega}_p \pm \Delta\omega)| = \varepsilon''_m(\tilde{\omega}_p \pm \Delta\omega)$, which gives $\Delta\omega = \omega_\tau/2$.

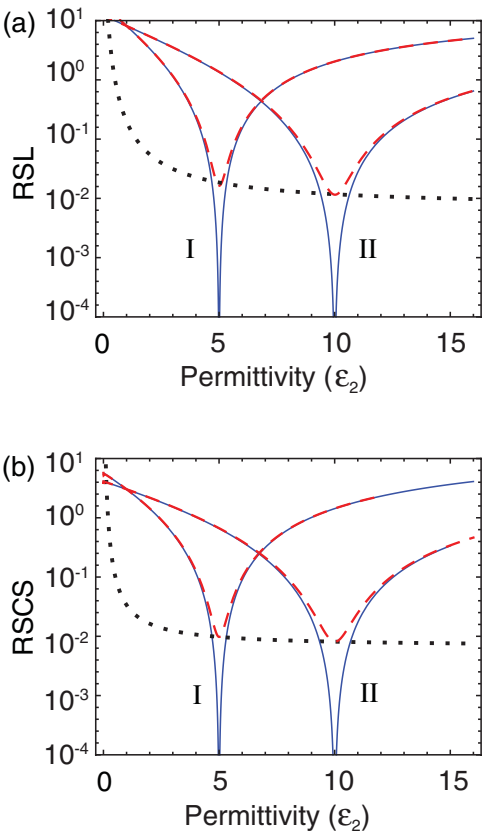

FIG. 2. (Color online) Relative scattering length (RSL) and cross section (RSCS) versus outer-shell permittivity for two-shell (a) cylindrically symmetric cloak and (b) spherically symmetric cloak with inner shell made of bulk silver. Two separate designs are being investigated in the case of cylindrical system: (I) $p_2 = 0.67$ and (II) $p_2 = 0.82$, and spherical system (I) $p_2 = 0.73$ and (II) $p_2 = 0.86$. The object permittivity is $\varepsilon_0 = 12$ and for all cases we use the optimal radii ratio $p_1 = 1/(1 + \sqrt{d})$. The limiting case as per Eq. (10) is presented with dotted (black) lines.

B. Composite media: Optical tunability

From the discussions in the previous section it is clear that while metal shells can be used to provide substantial reduction in scattering at the respective modified plasma frequencies their response cannot be tuned to operate across a broader spectral range. However, such tunability can be achieved using nanocomposite materials realized by embedding metal inclusions of permittivity ε_m in a dielectric host with permittivity ε_h.[1,12,22] If the inclusions are randomly oriented ellipsoids

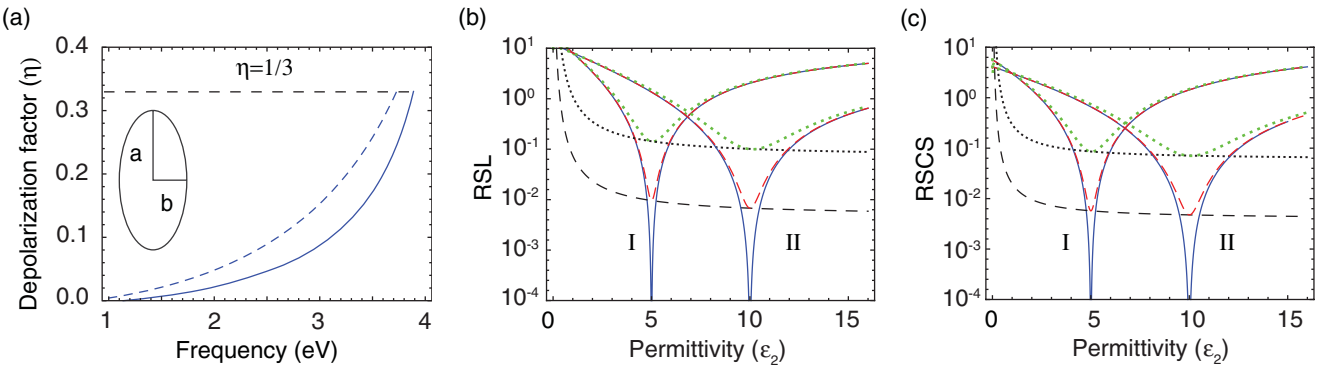

FIG. 3. (Color online) (a) Depolarization factor for composite host materials $\varepsilon_h = 1$ (solid line) and $\varepsilon_h = 2.0$ (dashed line) at different frequencies and $f = 0.05$. RSL and RSCS) versus outer-shell permittivity of two-shell (b) cylindrically symmetric cloaking system and (c) spherically symmetric cloaking system, respectively. The composite inner shell is designed with two different hosts, $\varepsilon_h = 1$ (dashed red line) and $\varepsilon_h = 2.0$ (dotted green line) at $\hbar\omega = 1.14$ eV. In the plots we also consider two separate shell designs; cylindrical system (I) $p_2 = 0.67$ and (II) $p_2 = 0.82$, and spherical system (I) $p_2 = 0.73$ and (II) $p_2 = 0.86$. The embeded object has permitivity $\varepsilon_0 = 12$ and for all cases we use the optimal shell radii ratio $p_1 = 1/(1+\sqrt{d})$. The ideal lossless cases are represented with solid (blue) lines. The limiting case [as per Eqs. (9) and (14)] is presented with horizontal (dotted and dashed) black lines for both the host media.

with small volume fraction f, the effective permittivity of the composite is given by the Maxwell-Garnett formula:[23–26]

$$\varepsilon_{\text{eff}} = \varepsilon_h + \frac{f}{3}\sum_{j=x,y,z}\frac{\varepsilon_h(\varepsilon_m - \varepsilon_h)}{\varepsilon_h + \eta_j(\varepsilon_m - \varepsilon_h)}, \tag{11}$$

where η_j are the depolarization factors of the ellipsoids satisfying the condition $\sum_{j=x,y,z}\eta_j = 1$. For prolate spheroids (needle shaped), i.e., ellipsoids with semiaxes $a > b = c$, the depolarization factor is given as

$$\eta_x = \eta = \frac{1-e^2}{e^2}\left[\frac{1}{2e}\ln\left(\frac{1+e}{1-e}\right) - 1\right], \tag{12}$$

where $e^2 = 1-(b/a)^2$ is the eccentricity.[24] The other two depolarization factors are equal and given by $\eta_y = \eta_z = (1-\eta)/2$.

To operate at reduced losses and simplify the design we consider only the ellipsoid's low-frequency resonance set by the condition $\varepsilon'_m(\omega) = -\varepsilon_h(1-\eta)/\eta$. The effective permittivity of the composite depends on the physical and geometrical properties of the spheroids, which allows for substantial flexibility in satisfying the transparency condition in Eq. (7). Since Eq. (11) is valid for small volume fractions, usually less than 5%, we study the effects due to change in the depolarization factor, i.e., the shape of the inclusions or the host material of the composite, or both. For small metal losses ($\varepsilon''_m/\varepsilon'_m \ll 1$), the depolarization factor that satisfies the transparency condition $\varepsilon'_{\text{eff}}(\omega_{op}) = 0$ can be written as

$$\eta = \frac{1}{1-\varepsilon'_m(\omega_{op})/\varepsilon_h} - \frac{f}{3}, \tag{13}$$

where ω_{op} is the operation frequency, and the depolarization factor must vary from $\eta = 0$ (needles) to $1/3$ (spheres). Concurrently, the operation frequency for a given depolarization factor is obtained as $\omega_{op} = \omega_p/\sqrt{\varepsilon_b - \varepsilon_h + 3\varepsilon_h/(3\eta + f)}$. We must note that Eq. (13) is only valid for $f > 6\varepsilon_h\varepsilon''_m/[(\varepsilon''_m)^2 + (\varepsilon_h - \varepsilon'_m)^2]$, and for lower concentrations the transparency condition cannot be satisfied ($\varepsilon'_{\text{eff}} > 0$).

The operation frequency range of the composite cloak is depicted in Fig. 3(a). For air as a host medium and tuning the depolarization factor of the ellipsoids the frequency range of operation is $\hbar\omega_{op} \in (1.14 - 3.89)$ eV. For the same ellipsoid volume fraction and glass as a host medium the operational frequency exhibits a redshift and is within the range $\hbar\omega_{op} \in (0.83 - 3.74)$ eV. Clearly, by varying the composite host material and ellipsoidal aspect ratio (depolarization factor), one can tune the operation frequency over large sections of the visible and near-infrared spectra. However, for low depolarization factors the spheroid aspect ratios become prohibitive pertaining to the design of the cloak (the physical size of the system should be smaller than the incident wavelength) and one should impose the restriction $1/3 \geqslant \eta > 1/10$, which corresponds to ellipsoid aspect ratios within the range $1 \leqslant a/b < 3$. This restriction is sufficiently weak enough to allow effective cloaking throughout the entire optical spectral range.

To estimate the RSL and RSCS of the composite cloak we rely on Eq. (9) with the substitution $\varepsilon'_m \to \varepsilon''_{\text{eff}}(\omega_{op})$, where the composite effective permittivity is obtained from Eq. (11) and (13) and is given as

$$\varepsilon_1 = i\varepsilon''_{\text{eff}}(\omega_{op}) = \frac{3\varepsilon_h^2}{f}\frac{i\varepsilon''_m}{(\varepsilon_h - \varepsilon'_m)^2}. \tag{14}$$

For the geometrically optimized design [with $p_1 = 1/(1+\sqrt{d})$], low frequency of operation, and strongly scattering objects ($\varepsilon_0 \to \infty$) the RSCS and RSL asymptotically approach the limit:

$$\sigma^d_{R,\min}(\omega_{op}) = \left(\frac{3\omega_\tau\omega_{op}\varepsilon_h^2}{f\omega_p^2}\right)^2\left(\frac{1+\sqrt{d}}{\sqrt{d}}\right)^4. \tag{15}$$

Figures 3(b) and 3(c) depict the RSCS and RSL versus the outer-shell permittivity (ε_2) for two-shell cylindrical and spherical cloaking systems with inner shells made of different metal dielectric composites. We also compare with the ideal case (nondispersive media) and include air (dotted line) and glass (dashed line) as the composite host materials. The

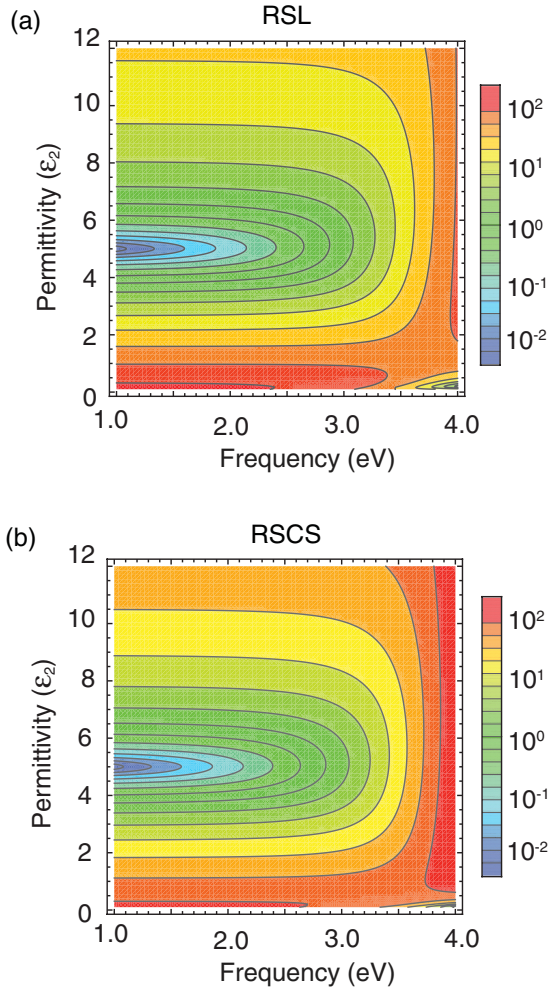

FIG. 4. (Color online) (a) RSL and (b) RSCS calculated as function of outer-shell permittivity (ε_2) and incident light frequency for a dielectric particle ($\varepsilon_0 = 12$) with $\varepsilon_h = 1$ and spheroids volume to surface fraction $f = 0.05$. The shells' radii ratios are (a) cylindrical system $(p_1, p_2) = (0.41, 0.67)$, and (b) spherical system $(p_1, p_2) = (0.37, 0.73)$.

operation frequency for all cases is set at $\hbar\omega = 1.14$ eV. A strong reduction in the scattering is observed, with the composite design based on air as a host media showing better performance [as expected by Eq. (15)]. Furthermore, a reduction of about 40% is observed as compared to the cloak designs based on bulk metal inner shells (see Fig. 2). Again, the minimal RSCS and RSL are obtained at outer-shell permittivity (ε_2) corresponding to the transparency condition Eq. (7). In the figures we also include the predicted geometrically optimized results as per Eqs. (9) and (14), which closely match the minimal values due to the exact calculations.

Finally, to provide a complete picture of the cloaks' performance, in Figs. 4(a) and 4(b) we vary the outer-shell permittivity (ε_2) and operational frequency (ω_{op}), respectively. A substantial decrease in the RSL and RSCS are observed across the entire optical and near-infrared spectral range. As predicted by Eq. (15), the scattering increases with increasing frequency to the point where the effect of the shell on the scattering cross section is no longer beneficial (for $\sigma^d_{R,\min} > 1$ and $\hbar\omega_{op} > 3.2$ eV). We should note that further decrease in scattering may be achieved by increasing the volume fraction of the spheroids provided the applicability of Eq. (11) is not violated.

IV. FULL WAVE ANALYSIS OF A GENERIC CYLINDRICAL CLOAK

The transparency condition Eq. (7) proposed in this work is valid for small objects, i.e., those whose physical size is much smaller than the wavelength of the impinging light. If the object size is comparable to the incident wavelength, the quasistatic analysis is no longer valid and the transparency condition is expected to fail. To study this transition and better understand the limiting system sizes of the design we perform a full wave analysis of a cylindrical two-shell cloak at optical and near-infrared frequencies.

We consider scattering of a plane transfer magnetic (TM) wave by an infinite two-shell cylindrical cloak as depicted in Fig. 1(b). The components of the incident H_z^i and scattered H_z^s magnetic fields outside the cloak assume the following well known general form:

$$H_z = H_z^i + H_z^s = H_0 \sum_{n=-\infty}^{\infty} i^n \left[J_n(k_e r) + S_n H_n^1(k_e r) \right] e^{in\phi}, \tag{16}$$

where J_n, H_n^1 are the Bessel and Henkel functions of the first kind, respectively, $k_e = (\omega/c)\sqrt{\varepsilon_e}$ is the wave vector in the host medium, and S_n are the scattering coefficients determined by applying the respective boundary conditions (see Appendix). The scattering cross-length is then given as a sum over all multipoles:[27–29]

$$\sigma = \frac{4}{k_e} \sum_{n=-\infty}^{\infty} |S_n|^2. \tag{17}$$

In the calculations, the geometrical parameters of the cloak are set at the optimal value $p_1 = 1/(1+\sqrt{d})$, $p_2 = 0.67$, and the shell permittivities are matched to the transparency condition in Eqs. (7) and (14). Figure 5 illustrates the RSL of the composite cloak, for cylindrical dielectric and metal particles serving as an object. As expected, for systems with small overall sizes [see Figs. 5(a) and 5(c)] a drastic reduction in scattering over the entire optical spectrum is achieved for $\varepsilon_2 = (1+p_2)/(1-p_2)$, thus reproducing the quasistatic result. Compared to a dielectric particle, a RSL across a broader frequency range is observed in the case of a metallic object. This is due to the dramatic enhancement of the metal particle scattering at the surface plasmon frequency $\hbar\omega_{sp} = \hbar\omega_p/\sqrt{\varepsilon_b + \varepsilon_e} = 3.71$ eV. However, as the system size increases [see Figs. 5(b) and 5(d)] the transparency condition in Eq. (7) is no longer sufficient to arrest the scattering process. This is an expected behavior since the contribution of the higher-order multipoles in the scattering cross-length for $k_e r_2 \ll 1$ increases with the physical size as (see Appendix)

$$S_n = \frac{i\pi}{\Gamma(n)\Gamma(n+1)} \left(\frac{k_e r_2}{2} \right)^{2n} \frac{\varepsilon_2\left(1-p_2^n\right) - \varepsilon_e\left(1+p_2^n\right)}{\varepsilon_2\left(1-p_2^n\right) + \varepsilon_e\left(1+p_2^n\right)}. \tag{18}$$

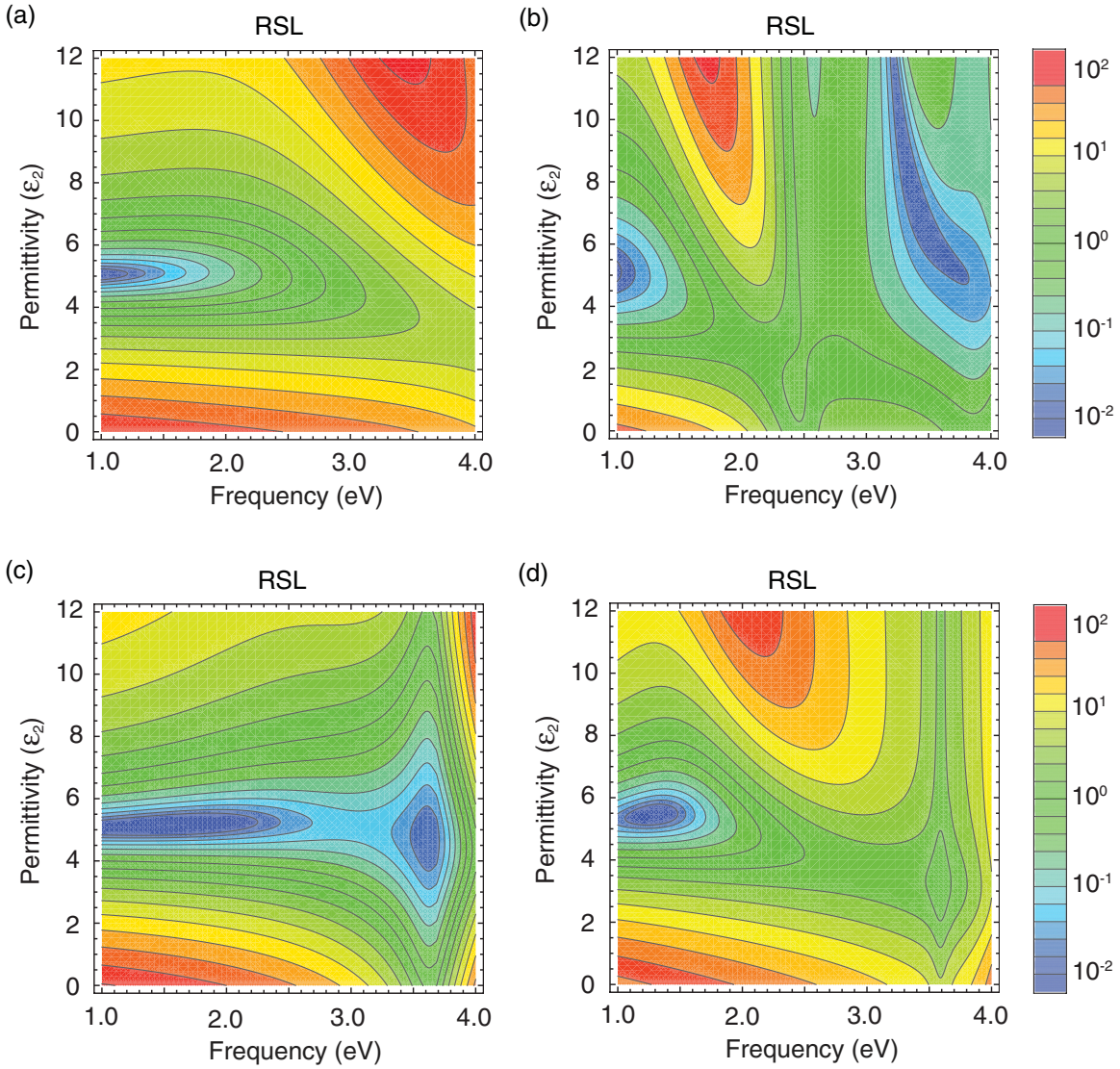

FIG. 5. (Color online) Full wave calculations of the RSL as a function of outer-shell permittivity (ε_2) and incident light frequency for dielectric particle $\varepsilon_0 = 12$ (a), (b) and metal particle (c), (d) enclosed in a cloaking system with radii $r_2 = 50$ nm (a), (c) and $r_2 = 100$ nm (b), (d).

It is straightforward to show that the quadruple scattering term of the cloak will overcome the dipolar term of the object for $k_e r_2 > \sqrt{8 p_1 (1 + p_2 + p_2^2)}$ (assuming $\varepsilon_0 \gg 1$). Overall, for particle diameters larger than 400 nm a substantial reduction in scattering and/or extinction cannot be expected in the optical spectral range.

Finally, we would like to address the generic property of our cloak design, namely its object independence. The condition $\varepsilon_{l-1} = 0$ leads to $\varepsilon_{\text{eff}}^{l-1} = 0$ [see Eq. (4)] regardless of the effective permittivity $\varepsilon_{\text{eff}}^{l-2}$ of the underlying shell or object substructure. This allows the design to cloak objects that are virtually arbitrary in shape and composition provided the objects are encapsulated by $l \geqslant 2$ shells.

To verify the generic properties of the cloak, full wave simulations using a finite-difference frequency domain (FDFD) software package (COMSOL MULTIPHYSICS) are performed. A metallic, rounded star-shaped object is placed inside the cloak. The permittivities of the shells are set at $\varepsilon_2 = 5$ and $\varepsilon_1 = 0$ with radii ratio $p_1 = 0.67$ ($r_2 = 106$ nm and $r_1 = 87$ nm). The system is illuminated by a TM polarized from a point source positioned 130 nm from the center of the object.

The magnetic field distribution is shown in Fig. 6. The cylindrical wave generated by the source smoothly bends around the cloaked region indicating reduced scattering [see Fig. 6(a)]. The phase fronts remain undisturbed as they exit the cloak and no shadow formation is noted. Figure 6(b) illustrates the magnetic field distribution when the cloak is removed. In this case the incident wave is strongly scattered and the phase fronts appear severely disturbed after traversing the object. The formation of shadows and presence of resonances within the object are clearly observed. The difference between the systems response shows that the cloak design based on the transparency condition Eq. (7) can considerably reduce scattering from objects with diverse optical and geometrical properties.

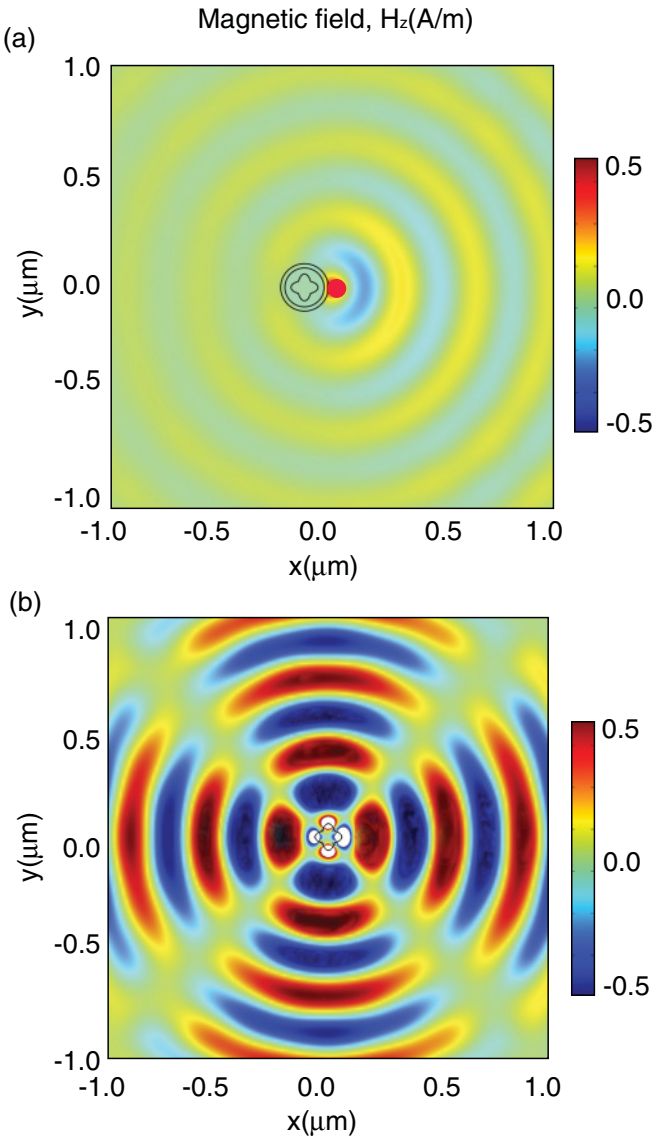

FIG. 6. (Color online) Full wave calculations of light scattering due to a point source in close proximity to a star-shaped metal object with (a), and without (b) the cloak. The incident TM wave has frequency $\hbar\omega = 3.8$ eV.

V. SUMMARY

In this work we propose a *generic cloaking system* based on zero-permittivity composite materials. The proposed analytical model and full wave calculations show that a dramatic suppression of dipolar scattering can be achieved for an arbitrary object enclosed within a multishell cloaking system. A reduction of scattering across the entire optical spectrum for dielectric objects using realistic shell materials is demonstrated. This study provides a direction for achieving optical invisibility without the use of metamaterials and also underlines the role of zero-index materials in the general phenomenon of optical transparency.

ACKNOWLEDGMENTS

We would like to thank Dr. S. G. Moiseev, K. Inturi, S. Animilli, Dr. N. Simicevic, Dr. A. Sihvola, and Dr. D. Robbins for useful discussions. This work has been supported by the Louisiana Board of Regents and NSF under Contracts No. LEQSF (2007-12)-ENH-PKSFI-PRS-01, No. LEQSF(2011-14)-RD-A-18, and No. NSF(2010)-PFUND-202.

APPENDIX

To calculate the scattering coefficients of the cloaking system shown in Fig. 1(b), we solve the Maxwell's curl equations in cylindrical coordinates. For an incident plane TM wave the components of the incident field (i), the field inside the mth shell, and scattered magnetic fields assume the following general form:

$$\begin{aligned} H_z^i &= H_0 \sum_{n=-\infty}^{\infty} i^n J_n(k_e r)\, e^{in\phi}, \\ H_z^{(m)} &= H_0 \sum_{n=-\infty}^{\infty} i^n \left[A_n^{(m)} J_n(k_m r) + B_n^{(m)} H_n^1(k_m r)\right] e^{in\phi} \\ H_z^s &= H_0 \sum_{n=-\infty}^{\infty} i^n S_n H_n^1(k_e r) e^{in\phi}, \end{aligned} \tag{A1}$$

where J_n, H_n^1 are the Bessel and Henkel functions of the first kind, respectively, k_e and k_m ($m = 0,1,2\cdots l$) are the wave numbers inside the cloak. $A_n^{(m)}$, $B_n^{(m)}$, S_n are the expansion coefficients with $B_n^{(0)} = 0$ at the origin. For an l-shell system, and applying boundary conditions, the scattering coefficients (for $\varepsilon_{l-1} = 0$) are given as

$$S_n^{\text{cloak}} = \frac{\alpha_n^l J_n(k_l r_{l-1}) + \beta_n^l H_n^1(k_l r_{l-1})}{\gamma_n^l J_n(k_l r_{l-1}) + \delta_n^l H_n^1(k_l r_{l-1})}, \tag{A2}$$

where $k_l = (\omega/c)\sqrt{\varepsilon_l}$ and coefficients

$$\begin{aligned} \alpha_n^l &= \varepsilon_l J_n'(k_e r_l) H_n^1(k_l r_l) - \varepsilon_e J_n'(k_l r_l) J_n(k_e r_l), \\ \beta_n^l &= \varepsilon_e J_n'(k_l r_l) J_n(k_e r_l) - \varepsilon_l J_n'(k_e r_l) J_n(k_l r_l), \\ \gamma_n^l &= \varepsilon_e H_n'^1(k_l r_l) H_n^1(k_e r_l) - \varepsilon_l H_n'^1(k_e r_l) H_n^1(k_l r_l), \\ \delta_n^l &= \varepsilon_l H_n'^1(k_e r_l) J_n(k_l r_l) - \varepsilon_e J_n'(k_l r_l) H_n^1(k_e r_l). \end{aligned} \tag{A3}$$

Here the prime corresponds to differentiation with respect to the radial coordinate and special care must be taken when considering the $n = 0$ term. Similarly, the scattering coefficients for the object are

$$S_n^{\text{obj}} = \frac{\varepsilon_e J_n'(k_0 r_0) J_n(k_e r_0) - \varepsilon_0 J_n'(k_e r_0) J_n(k_0 r_0)}{\varepsilon_0 H_n'^1(k_e r_0) J_n(k_0 r_0) - \varepsilon_e J_n'(k_0 r_0) H_n^1(k_e r_0)}. \tag{A4}$$

In the quasistatic limit $k_l r_l \ll 1$, Eqs. (A2) and (A4) are reduced to

$$\begin{aligned} S_n^{\text{cloak}} &= \frac{i\pi}{\Gamma(n)\Gamma(n+1)} \left(\frac{k_e r_l}{2}\right)^{2n} \\ &\quad \times \left\{ \frac{\varepsilon_l\left(1 - p_l^n\right) - \varepsilon_e\left(1 + p_l^n\right)}{\varepsilon_l\left(1 - p_l^n\right) + \varepsilon_e\left(1 + p_l^n\right)} + O[(k_e r_l)^2] \right\}, \\ S_n^{\text{obj}} &= \frac{i\pi}{\Gamma(n)\Gamma(n+1)} \left(\frac{k_e r_0}{2}\right)^{2n} \left\{ \frac{\varepsilon_0 - \varepsilon_e}{\varepsilon_0 + \varepsilon_e} + O[(k_e r_0)^2] \right\}. \end{aligned} \tag{A5}$$

Considering the dipolar term ($n = 1$) we derive the second transparency condition for the cloak

$$\varepsilon_l = \varepsilon_e \frac{1 + p_l}{1 - p_l}, \tag{A6}$$

which coincides with Eq. (7b) for $d = 2$. We must note that an arbitrary multipole (n) can also be eliminated from the far field provided

$$\varepsilon_l = \varepsilon_e \frac{1 + p_l^n}{1 - p_l^n}. \tag{A7}$$

*dgenov@latech.edu

[1] W. Cai, U. K. Chettiar, A. V. Kildishev, and V. M. Shalaev, Nat. Photonics **1**, 224 (2007).
[2] S. A. Cummer, B. I. Popa, D. Schurig, D. R. Smith, and J. Pendry, Phys. Rev. E **74**, 036621 (2006).
[3] U. Leonhardt, Science **312**, 1777 (2006).
[4] J. B. Pendry, D. Schurig, and D. R. Smith, Science **312**, 1780 (2006).
[5] U. Leonhardt and T. Philbin, *Geometry and Light: The Science of Invisibility* (Dover, New York, 2010).
[6] U. Leonhardt and T. Philbin, New J. Phys. **8**, 247 (2006).
[7] Y. Lai, H. Chen, Z.-Q. Zhang, and C. T. Chan, Phys. Rev. Lett. **102**, 093901 (2009).
[8] J. B. Pendry and S. A. Ramakrishna, J. Phys.: Condens. Matter **14**, 8463 (2002).
[9] H. Chen, C. T. Chan, and P. Sheng, Nat. Mater. **9**, 387 (2010).
[10] M. W. McCall, A. Favaro, P. Kinsler, and A. Boardman, J. Opt. **13**, 024003 (2011).
[11] D. Schurig, J. Mock, B. Justice, S. Cummer, J. Pendry, A. Starr, and D. Smith, Science **314**, 977 (2006).
[12] Y. Huang, Y. Feng, and T. Jiang, Opt. Express **15**, 11133 (2007).
[13] A. Alù and N. Engheta, Phys. Rev. E **72**, 016623 (2005).
[14] M. Kerker, J. Opt. Soc. Am. **65**, 376 (1975).
[15] X. Zhou and G. Hu, Phys. Rev. E **74**, 026607 (2006).
[16] J. Valentine, S. Zhang, T. Zentgraf, E. Ulin-Avila, D. Genov, G. Bartal, and X. Zhang, Nature **455**, 376 (2008).
[17] N. Fang, H. Lee, C. Sun, and X. Zhang, Science **308**, 534 (2005).
[18] Y. Lai, J. Ng, H. Y. Chen, D. Z. Han, J. J. Xiao, Z. Q. Zhang, and C. T. Chan, Phys. Rev. Lett. **102**, 253902 (2009).
[19] D. A. Genov, S. Zhang, and X. Zhang, Nat. Phys. **5**, 687 (2009).
[20] G. W. Milton and N.-A. P. Nicorovici, Proc. R. Soc. A **462**, 3027 (2006).
[21] *Handbook of Optical Constants of Solids*, edited by E. D. Palik (Academic, New York, 1985).
[22] N. Garcia, E. V. Ponizovskaya, and J. Q. Xiao, Appl. Phys. Lett. **80**, 1120 (2002).
[23] D. J. Bergman and D. Stroud, Solid State Phys. **46**, 147 (1992).
[24] D. A. Genov, A. K. Sarychev, and V. M. Shalaev, J. Nonlinear Opt. Phys. Mater. **12**, 419 (2003).
[25] J. C. Maxwell-Garnett, Philos. Trans. R. Soc. London **203**, 385 (1904).
[26] D. Polder and J. Vansanteen, Physica **12**, 257 (1946).
[27] C. Bohren and D. Huffman, *Absorption and Scattering of Light by Small Particles* (Wiley, New York, 1998).
[28] M. Kerker and E. Matijevi, J. Opt. Soc. Am. **51**, 506 (1961).
[29] G. Mie, Ann. Phys. **330**, 377 (1908).